Chemical Papers (2023) 77:2947–2956
https://doi.org/10.1007/s11696-023-02676-9

ORIGINAL PAPER

Green synthesis of silver nanoparticles using *Eupatorium adenophorum* leaf extract: characterizations, antioxidant, antibacterial and photocatalytic activities

Tarun Kumar Dua[1] · Simran Giri[1] · Gouranga Nandi[1] · Ranabir Sahu[1] · Tapan Kumar Shaw[2] · Paramita Paul[1]

Received: 26 September 2022 / Accepted: 13 January 2023 / Published online: 25 January 2023

Abstract
The green synthesis of metallic nanoparticles has tremendous impacts in various fields as found in recent years due to their low cost, easy and environmentally friendly synthesis. In this article, we report a simple and eco-friendly method for the synthesis of silver nanoparticles (AgNPs) using an aqueous *Eupatorium adenophorum* (*E. adenophorum*) leaf extract as a bioreductant. Interestingly, Fourier transform infrared (FTIR) spectroscopy analysis established that the *E. adenophorum* extract not only served as a bioreductant but also acted as a capping agent to stabilize the nanoparticles by functionalizing the surfaces. Various characterization techniques were adopted, such as X-ray powder diffraction (XRD), FTIR, ultraviolet–visible absorption (UV–Vis) spectroscopy, dynamic light scattering, scanning electron microscopy and energy-dispersive X-ray spectroscopy (EDX) to analyze the biosynthesized AgNPs. Biosynthesized nanoparticles were also explored for antioxidant, antibacterial and photocatalytic activities. The AgNPs showed improved free radical scavenging activity (IC_{50} 48.96 ± 0.84 µg/mL) and bacterial inhibitory effects against both gram-positive (*Staphylococcus aureus*; 64.5 µg/mL) and gram-negative (*Escherichia coli*; 82.5 µg/mL) bacteria. Photocatalytic investigation showed AgNPs were effective at degrading rhodamine dye (78.69% in 90 min) when exposed to sunlight. These findings collectively suggest that *E. adenophorum* AgNPs were successfully prepared without the involvement of any hazardous chemical and it may be an effective antibacterial, antioxidant and promising agent for the removal of hazardous dye from waste water produced by industrial dyeing processes.

Keywords *Eupatorium adenophorum* · Green synthesis · Silver nanoparticles · Antioxidant activity · Photocatalytic activity

Introduction

Nanomaterials are becoming more significant as a means of addressing material science issues. Preparation of nanosized silver nanoparticles (AgNPs) is one of the most promising fields of nanotechnology. Green synthesis of silver-based nanoparticles has been accomplished using a variety of physical, chemical and biological approaches (Lombardo et al. 2016; Treshchalov et al. 2017). Many research fields focus on green chemistry to improve and/or safeguard our global environment. Silver nanoparticles' applications are extensive, from food processing, cosmetics, home cleaning, catalytic and garment production to medicinal applications (Bansod et al. 2015; Benn et al. 2010; Zhu et al. 2022). Medicinally AgNPs have been used for the treatment of diseases such as cancer, HIV, diabetes, malaria and tuberculosis (Casañas Pimentel et al. 2016; Kalmantaeva et al. 2020; Kasithevar et al. 2017; Muthukumaran et al. 2015). Green chemistry-based strategies have been addressed in the synthesis of nanoparticles in recent years, among the various chemical and physical ways of nanoparticle synthesis (Noah and Ndangili 2022). When plant extracts are used to reduce and stabilize silver nanoparticles, they do not contain any synthetic chemical compounds on their surface. They are not toxic to human and the environment (Tamuly et al. 2013). The phytochemicals sticking to the surface of nanoparticles

✉ Paramita Paul
paramita37@gmail.com

[1] Department of Pharmaceutical Technology, University of North Bengal, Raja Rammohunpur, P.O. NBU, Darjeeling, West Bengal 734013, India

[2] Departmen of Pharmaceutical Technology, JIS University, Kolkata, West Bengal, India

are responsible for the scavenging effect of AgNPs against free radicals (Ansar et al. 2018).

Eupatorium adenophorum Spreng. (*E. adenophorum*) [also known as *Ageratina adenophora* (Spreng.)] of Asteraceae family, have been used in traditional medicine for the treatment of wounds, diabetes, inflammation, fever, jaundice and dysentery (Awah et al. 2012; Giri et al. 2022; Sharma et al. 1998; Tiwary et al. 2015; Uprety et al. 2011). It is well known that consummation or even exposure of the plant has serious adverse effects on humans as well as animals, due to presence of toxins (sesquiterpenes) (Cui et al. 2021; Ren et al. 2021). However recent investigations have shown that some extracts and/or isolated secondary metabolites are safe for use and possess considerable antioxidant, antifungal and/or medicinal properties. Sesquiterpenoids, triterpenes, flavonoids, phenolics, coumarins, steroids and phenylpropanols have been isolated and identified from *E. adenophorum* (Liu et al. 2021). Various pharmacological studies revealed that *E. adenophorum* extract had antimicrobial (Manandhar et al. 2019), antioxidant (Lallianrawna et al. 2013), anticancer (Mani et al. 2019), wound healing (Garg and Paliwal 2011), analgesic (Mandal et al. 2005), antipyretic (Ringmichon and Gopalkrishnan 2017), anti-inflammatory (Shi et al. 2019) activities and antiviral activity against COVID-19 main protease (Neupane et al. 2021).

The present work aimed to explore *E. adenophorum*'s potential for the first time in the synthesis of AgNPs. X-ray powder diffraction (XRD), Fourier transform infrared spectroscopy (FTIR), ultraviolet–visible absorption (UV–Vis) spectroscopy, dynamic light scattering (DLS) and scanning electron microscopy (SEM) were used to analyze the biosynthesized AgNPs. Biosynthesized nanoparticles were also studied for antioxidant, antibacterial and photocatalytic activities.

Materials and methods

Materials

Silver nitrate ($AgNO_3$) and Rhodamine B were procured from Sisco Research Laboratory, Mumbai, India. 2,2-Diphenyl-1-picrylhydrazyl (DPPH) and Mueller Hinton Broth (MHB) were supplied by HiMedia (Mumbai, India). All other chemicals and reagents used were of highly pure analytical grade.

Leaves of *E. adenophorum* were collected from Jaigaon, Alipurduar, West Bengal, in March 2022. The plant was authenticated (Reference no. CNH/Tech.II/2021/11) by the Botanical Survey of India, Shibpur, Howrah (West Bengal). This plant specimen has been preserved in the laboratory for further reference.

Preparation of plant extract

The collected *E. adenophorum* leaves were washed thoroughly with distilled water several times to remove dust and dried under shade. The dried leaves were ground to get fine powder, and its aqueous extract was prepared using the Soxhlet apparatus. The extracts were filtered to remove particulate matter and lyophilized using lyophilizer (Cool-Safe, Labogene, Allerod, Denmark) to yield the powdered (amorphous) crude extracts.

Preparation of *E. adenophorum* silver nanoparticles

Green synthesis method is used to synthesize AgNPs with slight modification (Kumar et al. 2014). *E. adenophorum* powdered extract (500 mg) was dissolved in 100 mL of distilled water (Fig. 1A). Then, 10 mL of the above extract was added to 90 mL of 0.1 M $AgNO_3$ solution in a conical flask and heated at the temperature range between 60 and 80 °C with continuous stirring in a magnetic stirrer at a speed of 400 rpm. The solution color turned brown, indicating the formation of AgNPs (Fig. 1B). The contents were centrifuged for 20 min at 10,000 rpm, and the precipitate was collected after discarding the supernatant. The collected AgNPs were dried in a freeze dryer without using a cryoprotector before being utilized for characterizations and antibacterial and antioxidant activities.

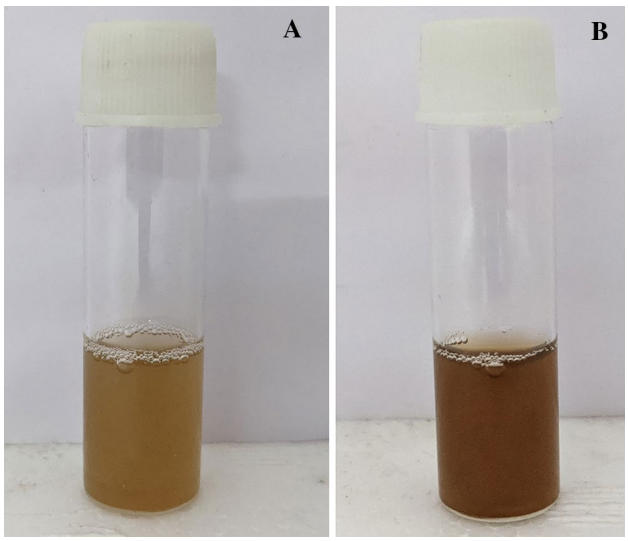

Fig. 1 *E. adenophorum* leaf extract (**A**) and formation of AgNPs by adding $AgNO_3$ in *E. adenophorum* leaf extract (**B**)

Characterizations of *E. adenophorum* silver nanoparticles

UV–visible spectrum for *E. adenophorum* silver nanoparticles

UV–visible spectral analysis was done by using Shimadzu UV–visible spectrophotometer (UV-1900i, UV visible spectrophotometer, Shimadzu, Japan). The analysis was carried out in a scan range of 800–200 nm with a resolution of 1 nm. Both the *E. adenophorum* leaf extract and the AgNPs synthesized from the leaf extract were scanned by UV–visible spectroscopy to confirm the formation of AgNPs. After completion of the reaction, one milliliter of the AgNPs sample was pipetted out and scanned at room temperature without dilution.

FTIR analysis for *E. adenophorum* silver nanoparticles

The dried sample extract and biosynthesized nanoparticles were individually mixed with the KBr powder and pressed into a pellet. The FTIR spectrum was recorded in the IR region of 4000–400 cm^{-1} on a compact FTIR Spectrometer (Bruker, alpha II spectrometer, USA).

X-ray diffraction (XRD) analysis for *E. adenophorum* silver nanoparticles

E. adenophorum silver nanoparticles were characterized to distinguish their crystal structure using X-ray diffraction technique. The XRD pattern was recorded using computer-controlled XRD system (Rigaku, Japan, SmartLab 9kW).

Particle size and zeta potential analysis of *E. adenophorum* silver nanoparticles

The particle size and zeta potential of *E. adenophorum* silver nanoparticles were determined using particle size analyzer (Litesizer 500, Anton Paar GmbH, Austria). In the present study, a small, weighed quantity of the experimental sample was dispersed in deionized water by vortex mixing followed by sonication for 1 h and placed in a disposable cuvette for determining average particle size. The Anton Paar's Omega cuvettes were used for zeta potential measurement by the use of the same prepared sample solution.

Scanning electron microscopy and energy-dispersive X-ray spectroscopy

Scanning electron microscopy (SEM) and energy-dispersive X-ray spectroscopy (EDX) were performed by using a scanning electron microscope (JEOL, Tokyo, Japan) with an accelerating voltage of 15 kV. The elemental composition of AgNPs was assessed using SEM fitted with an EDX (OXFORD) detector.

Antioxidant activity

The ability of AgNPs to scavenge DPPH radical was determined according to the method of Mensor et al. with a slight modification (Mensor et al. 2001). In brief, 2 mL of AgNPs solution in water was mixed with 1 mL of DPPH solution (0.3 mM) at various concentrations (5, 10, 25, 50, 75 and 100 µg/mL). To make the control, 1 mL of DPPH was mixed with 2 mL of water. The reaction's absorbance was measured at 517 nm after 30 min. Distilled water served as the blank. The percentage of DPPH radical scavenging was estimated using the following formula.

$$\%\ \text{DPPH radical scavenging activity} = \left[(\text{Ac} - \text{As})/\text{Ac}\right] \times 100$$

where Ac and As are the absorbance of the control and the sample, respectively.

Antibacterial activity of *E. adenophorum* silver nanoparticles

The antibacterial assays were done on human pathogenic *Escherichia coli* (*E. coli)* and *Staphylococcus aureus* (*S. aureus*). By using the broth dilution method, the minimum inhibitory concentration (MIC) was ascertained (Wiegand et al. 2008). Mueller Hinton Broth (MHB) was used for bacterial strains. Fresh cultures at 10^6 CFU/mL were added to each tube of sterile MHB. Then, AgNPs was loaded at different concentrations (10, 20, 30, 40, 50, 60, 70, 80, 90, 100, 110 and 120 µg/mL). In the experiment, broth and inoculum served as the positive control, whereas broth and AgNPs and broth alone served as the negative control. For 16–24 h, the bacteria-inoculated tubes were incubated at 37 °C. To obtain the MIC, the absorbance was measured at 600 nm. The MIC was the lowest concentration with above 90% inhibition.

Photocatalytic activity

For measurement of catalytic activity of biosynthesized AgNPs we carried out the degradation and reduction of Rhodamine B (Baruah et al. 2019). AgNPs' photocatalytic activity was calculated in visible light using Rhodamine B dye. The degradation of Rhodamine B was also performed in absence of AgNPs with leaf extract and without leaf extract. To reach equilibrium between absorption and desorption, the reaction mixture was agitated for 20 min in the dark. Five milligrams of the nanoparticles was added to 10 mg/L of Rhodamine B solution, while the mixture was still being stirred in the presence of sunlight. At intervals of 15, 30, 45, 60, 75 and 90 min after starting the reaction under sunlight,

the reaction mixtures' maximum absorbance was measured by using a spectrophotometer to study its degradation. The rate of dye degradation (%) was calculated using the formula below.

$$\text{Dye degradation rate}\,(\%) = \left[\left(C_0 - C_t\right)/C_0\right] \times 100$$

where C_0 represents the starting concentration of rhodamine solution and C_t represents the concentration of dye solution following "t" hours of exposure to sunlight.

Results and discussion

Green synthesis of *E. adenophorum* silver nanoparticles

In this study, we have synthesized *E. adenophorum* silver nanoparticles using green approach. In this work, reduction of $AgNO_3$ was achieved by constituents of *Eupatorium adenophorum* leaf aqueous extract with application of temperature in the range of 60–80 °C with continuous stirring. The formation of AgNPs was indicated by the color change from straw yellow to brown. Similar observations were reported by other investigators who used plant extracts as a reducing agent (Jayapriya et al. 2019). Based on the study by Rajput and team (Rajput et al. 2020), the temperature of the solution was maintained at a temperature more than 60 °C to get optimum particle size (*E. adenophorum*). Many studies showed that synthesis of smaller size AgNPs using other plant leaf extracts occurs when the reaction is performed at higher temperature (Alharbi et al. 2022; Kumar et al. 2018; Verma and Mehata 2016). AgNPs of particle size 51 nm were also synthesized in the presence of sunlight by green approach using $AgNO_3$ and *Rivina humilis* leaf extract (Raghava et al. 2021). However, recently AgNPs were synthesized by the green method using *E. adenophorum* without applying heat during the reaction, and AgNPs formed were dried using hot air oven (Gautam et al. 2021). They report that the nanoparticles obtained were face-centered cubic geometry based on XRD data having particle size mostly of 24 nm estimated using the Debye-Scherrer equation (Gautam et al. 2021). In the present work, the particle morphology was characterized using SEM image, and average sizes were obtained using Litesizer.

UV–visible spectroscopy

The formation of AgNPs of silver nitrate containing *E. adenophorum* extract was confirmed by observing a visible color change from light brown to dark brown. The synthesized AgNPs shown in Fig. 2 was confirmed by the final solution's constant λ_{max} at 400 nm.

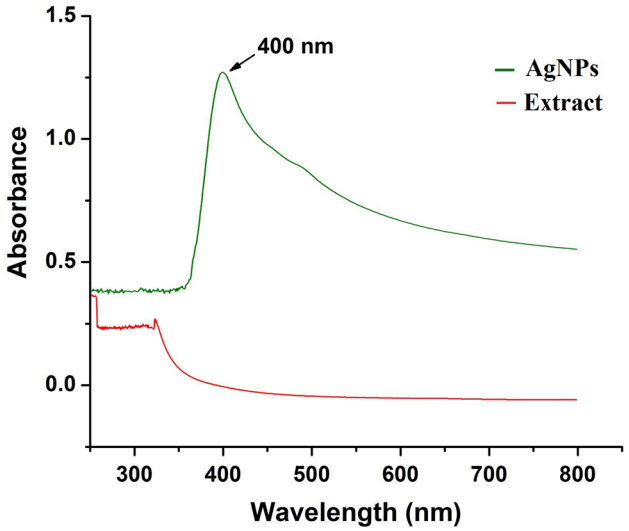

Fig. 2 UV–Vis spectra of *E. adenophorum* leaf extract and AgNPs synthesized using *E. adenophorum* leaf extract

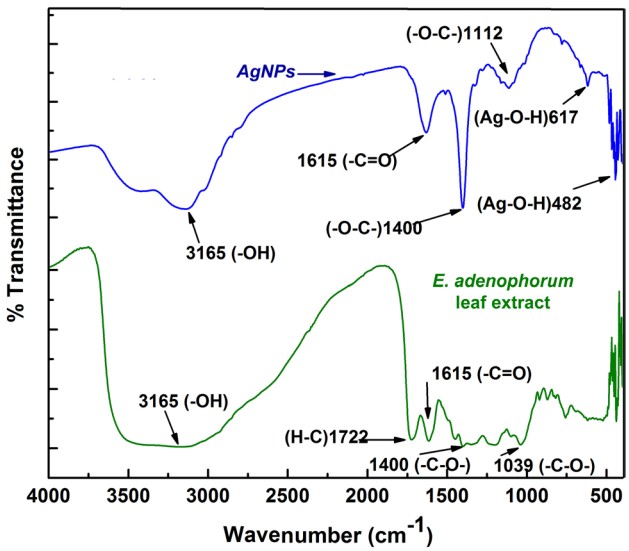

Fig. 3 FTIR spectroscopy analysis of *E. adenophorum* leaf extract and AgNPs

FTIR analysis for *E. adenophorum* silver nanoparticles

FTIR spectrometry of the aqueous extract of *E. adenophorum* leaves and AgNPs produced with *E. adenophorum* leaf extract is shown in Fig. 3. The FTIR spectra obtained from extract showed different characteristic peaks at 3165 cm^{-1} for –OH stretching vibration, at 1722 cm^{-1} for –C–H stretching vibration, at 1615 cm^{-1} for –C=O stretching of –COOH group of polyphenols, at 1400 cm^{-1} and 1039 cm^{-1} for –C–O stretching vibration. These characteristic peaks

substantiate the presence of polyphenolic compounds in the extract, which might act as bioreductant in the formation of AgNPs through reduction of silver nitrate. The FTIR spectra obtained from AgNPs showed characteristic peaks at 3165 cm^{-1}, 1615 cm^{-1} and 1400 cm^{-1} for –OH stretching, –C=O and –O–C– stretching vibration, which indicates the presence of polyphenolic compounds at the surfaces of nanoparticles. Another peak at 1112 cm^{-1} was observed for –C–O stretching. The peaks at 617 cm^{-1} and 482 cm^{-1} were assigned to –O–H bond between oxygen atom of Ag_2O and H-atom of phenolic compound at the surface of nanoparticles, which indicates the formation of AgNPs.

X-ray diffraction (XRD) analysis for *E. adenophorum* silver nanoparticles

On examining XRD pattern (Fig. 4) of AgNPs, the prominent peaks at $2\theta = 38.030°$, 44.214°, 64.354°, 77.267° and 81.299° represent the (111), (200), (220), (311) and (222) Bragg's reflections of the face-centered cubic structure of silver, respectively. It confirmed the crystalline structure of AgNPs synthesized using *E. adenophorum* leaf extract. The preferred direction of the growth of the silver nanoparticles was indicated by the most intense peak, which falls within the (111) plane. The phase purity of the material as synthesized was simply verified by the absence of any other peaks. The highly crystalline structure of the silver nanoparticles as synthesized was clearly indicated by the sharp and strong peaks.

Particle size and zeta potential analysis of *E. adenophorum* silver nanoparticles

From the particle size graph, the average particle size of the AgNPs obtained was 117.75 nm (Fig. 5A). The particles obtained were as small as 30 nm and as large as 400 nm. The

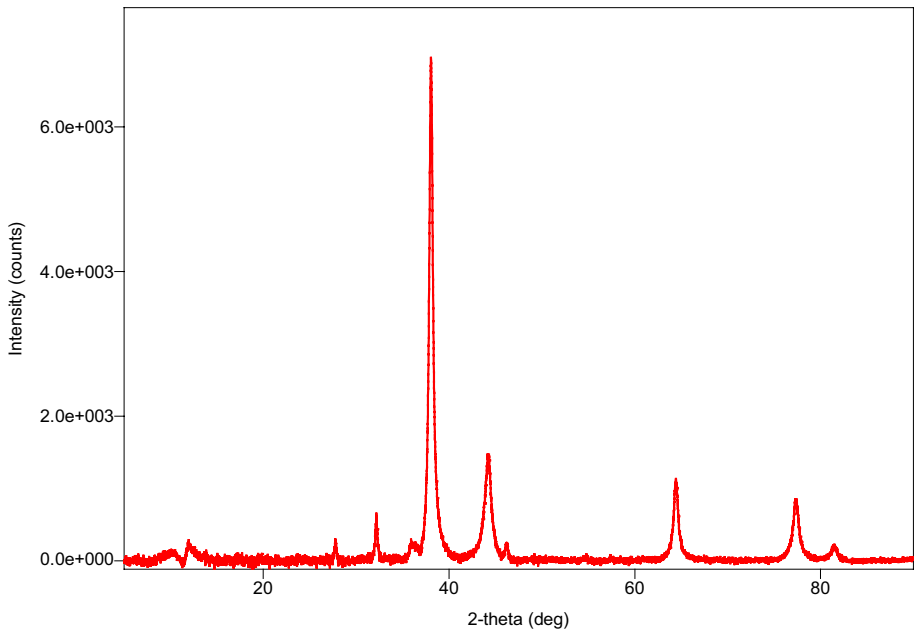

Fig. 4 XRD pattern of AgNPs synthesized using *E. adenophorum* leaf extract

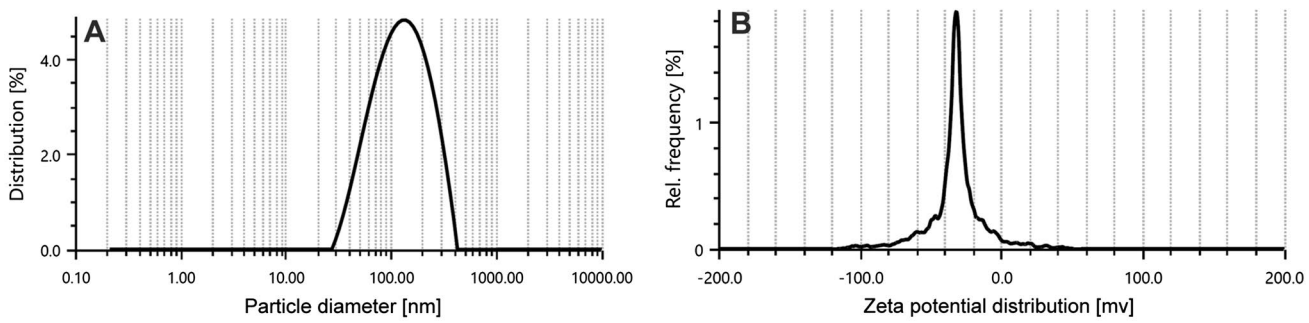

Fig. 5 Zetasizer measurement of the average particle size of AgNPs synthesized using *E. adenophorum* leaf extract (**A**) and zetapotential of AgNPs (**B**)

zeta potential is a property of nanoparticles that quantifies charge. It measures the electrical charge that a nanoparticle has on its surface. The zeta potential provides information about the stability of the particles. Figure 5B displays the zeta potential distribution graph. The zeta potential of *E. adenophorum* AgNPs was found to be − 33.4 mV (Fig. 5B). The zeta potential is negative, which denotes repulsion and increased stability in colloidal state.

Scanning electron microscopy (SEM)

The SEM image of the biosynthesized AgNPs (Fig. 6) indicates the presence of extremely tiny, spherical nanoparticles. Particle aggregation is also depicted in the illustration. The evaporation of solvent during sample preparation may cause AgNPs to aggregate. Additionally, the formation of aggregation of AgNPs was due to freezing without cryoprotectants which in turn induce stress from the formation of ice crystals. This might have caused the particle size variance.

The EDX profile confirmed that the particles were AgNPs by displaying a high silver signal and remarkably stronger peaks. The presence of carbon in the EDX image (Fig. 7) substantiates the presence of carbon compound on the surface of the particles, which might be phytoconstituents present in the plant extract. Thus, EDX data confirm the formation of AgNPs using *E. adenophorum* extract.

Antioxidant activity

The DPPH radical is a free radical with one electron and a relatively stable structure (Priyadarsini et al. 2003). The color of the solution changes when it comes into contact with a scavenger. The scavenging efficacy of AgNPs on DPPH radical was significantly linked with concentration, as shown in Fig. 8. The DPPH radical scavenging experiment showed

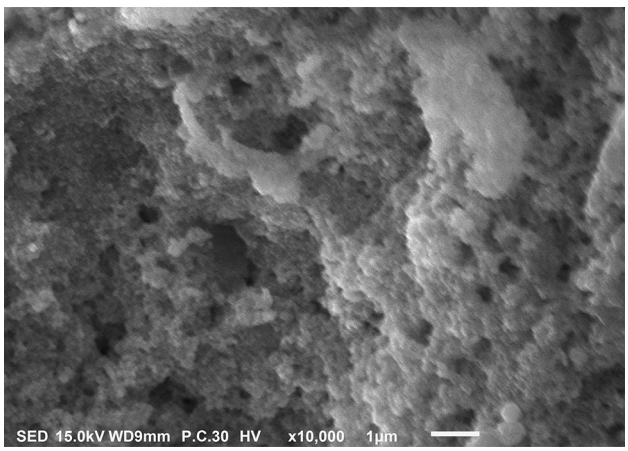

Fig. 6 SEM image of AgNPs synthesized using *E. adenophorum* leaf extract

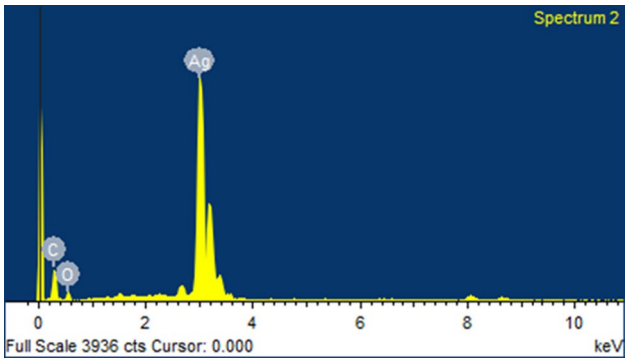

Fig. 7 EDX spectrum of AgNPs with a higher percentage of the silver signal

that AgNPs had significant radical scavenger characteristics, with an IC_{50} value of 48.96 ± 0.84 µg/mL (Fig. 8) when compared to ascorbic acid's IC_{50} value of 14.35 ± 0.16 µg/mL. Previous studies reported the IC_{50} value of 92.791 µg/mL of methanolic extract of *E. adenophorum* (Khazeo et al. 2018). The DPPH activity of the synthesized AgNPs was found to increase in a dose-dependent manner.

Antibacterial activity

The silver nanoparticles' minimum inhibitory concentrations (MIC) against the gram-negative bacteria *E. coli* and the gram-positive bacteria *S. aureus* were determined to be 82.5 µg/mL and 64.5 µg/mL, respectively. The antibacterial activity of AgNPs is connected due to any of the four mechanisms. Firstly, AgNPs interact directly with the bacterial cell membrane, leading to subsequent membrane damage and the formation of complexation with the cellular components. Secondly, AgNPs adhere to the surface of cell membrane and wall and cause damage there. Thirdly, AgNPs interact with thiol (−SH) groups and induce the formation of reactive oxygen species (ROS) in the cells that cause oxidative stress. Lastly, AgNPs modulate the signal transduction pathways (Kung et al. 2018; Rai et al. 2014). The spherical AGNPs showed promising and powerful antibacterial activity although might be less that cuboid- or triangular-shaped AgNPs (Baghbani-Arani et al. 2017; Dakal et al. 2016; Qing et al. 2018). AgNPs with smaller size (10–50 nm) are more effective in terms of their biocompatibility, stability and enhanced antimicrobial activity (Dakal et al. 2016). The nanoparticles were of different sizes starting from 27 nm. Hence, prepared nanoparticles could able to prevent bacterial infection effectively.

Photocatalytic activity

To determine catalytic activity, Rhodamine B was employed as an experimental probe. This well-known

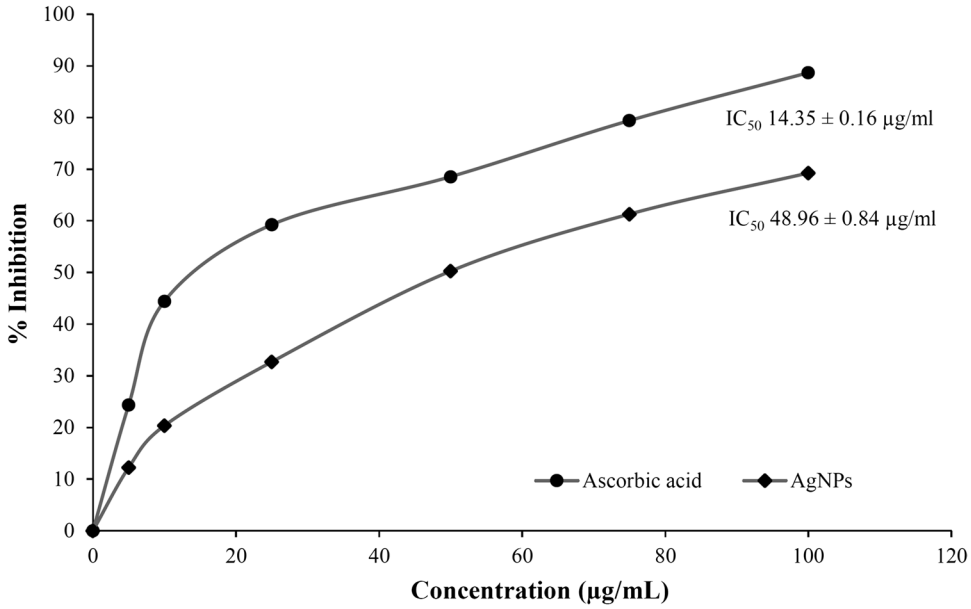

Fig. 8 DPPH radical scavenging activity of ascorbic acid and AgNPs synthesized using *E. adenophorum* leaf extract

water-soluble color is utilized in various industrial fields, including textile, leather, printing, paper and pharmaceuticals. Under sunlight, the photocatalytic activity of AgNPs was calculated. To minimize the impact of light, Rhodamine B was used as a control in the absence of a catalyst because it displayed a clear absorption spectrum at 554 nm. A gradual reduction in the absorption peak at 554 nm represents the reduction and degradation of Rhodamine B, as shown in Fig. 9A. This decline in the absorption peak clearly illustrates the catalytic activity of nanoparticles and the conversion of Rhodamine B to a colorless solution. Figure 9B, C shows the experimental result of the degradation of the Rhodamine B without AgNPs and without the AgNPs but containing the leaf extract. The result depicts no significant degradation of Rhodamine B in the absence of AgNPs or in the presence of only leaf extract without AgNPs. It was also noticed when Rhodamine B was treated with AgNPs, the rate of photodegradation of the dye increased with time (Fig. 9D). Rhodamine B dye showed time-dependent photodegradation, which was followed by a significant photodegradation (78.69%) with decolorization after 90 min. Previous studies showed 93% degradation achieved in 216 h (Awad et al. 2021). When compared photocatalytic activity at 90 min, 81.12% (Alshehri and Malik 2020) and 86.51% (Shaikh et al. 2020) degradation of Rhodamine B was reported under UV radiation in their studies. The Ln (C_t/C_0) versus time plot from Rhodamine B is shown in Fig. 9E. Rhodamine B's calculated degradation rate constant is 1.56×10^{-2}/min. The reaction process followed pseudo-first-order kinetics, as evidenced by the fact that Ln (C_t/C_0) value decreased over time.

Conclusion

Aqueous leaf extract from *E. adenophorum* was utilized successfully to synthesized silver nanoparticles where the extract plays a dual role as bioreductant and capping agent. In addition to showing bacterial inhibitory effects against human infections that were comparable to those of amoxicillin, the AgNPs also showed improved free radical scavenging activity. According to the results of the photocatalytic investigation, *E. adenophorum* AgNPs were effective at degrading rhodamine dye when exposed to sunlight. As a result, the textile and water purification sectors can greatly benefit from this. Our results clearly support the idea that plant-mediated nanoparticles can be employed in the near future for the treatment of diseases caused by free radicals as well as the purification of waste water be removing hazardous dye from waste water, in addition to being used as effective therapeutic agents against human pathogens.

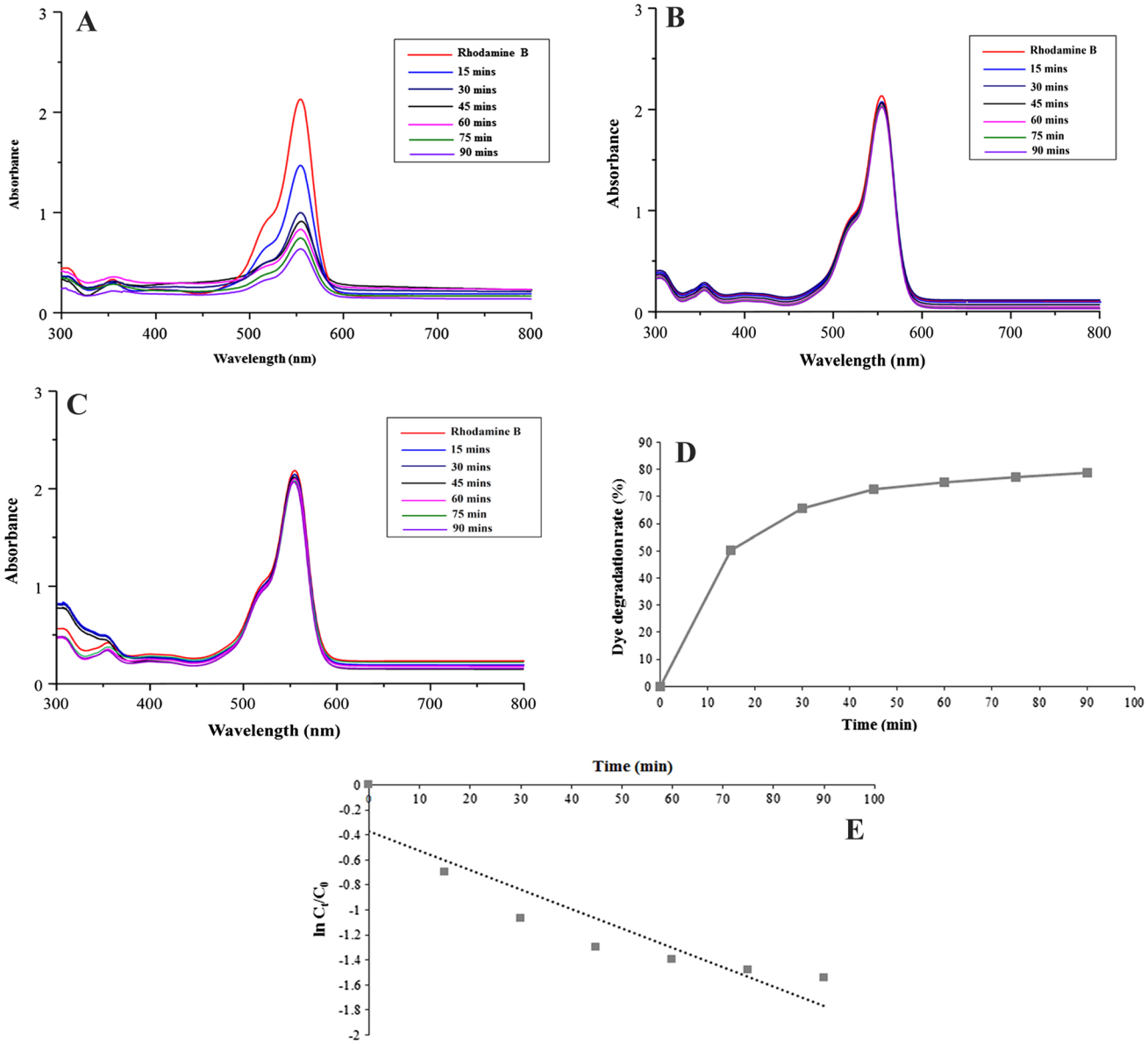

Fig. 9 Photocatalytic activity showing degradation of Rhodamine B by AgNPs (**A**), without AgNPs (**B**), with the leaf extract but without the AgNPs (**C**). Degradation rate of Rhodamine B by AgNPs (**D**), and kinetic plot of degradation of Rhodamine B by AgNPs (**E**)

Acknowledgements The authors sincerely acknowledge the University of North Bengal, West Bengal, India.

Funding Not applicable.

Declarations

Conflict of interest The authors declare that they have no competing interests.

References

Alharbi NS, Alsubhi NS, Felimban AI (2022) Green synthesis of silver nanoparticles using medicinal plants: characterization and application. J Radiat Res Appl Sci 15(3):109–124

Alshehri AA, Malik MA (2020) Phytomediated photo-induced green synthesis of silver nanoparticles using *Matricaria chamomilla* L. and its catalytic activity against rhodamine B. Biomolecules 10(12):1604

Ansar S, Abudawood M, Alaraj AS, Hamed SS (2018) Hesperidin alleviates zinc oxide nanoparticle induced hepatotoxicity and oxidative stress. BMC Pharmacol Toxicol 19(1):1–6

Awad MA, Hendi AA, Ortashi KM, Alzahrani B, Soliman D, Alanazi A, Alenazi W, Taha RM, Ramadan R, El-Tohamy M (2021) Biogenic synthesis of silver nanoparticles using *Trigonella*

foenum-graecum seed extract: characterization, photocatalytic and antibacterial activities. Sens Actuators A 323:112670
Awah FM, Uzoegwu PN, Ifeonu P, Oyugi JO, Rutherford J, Yao X, Fehrmann F, Fowke KR, Eze MO (2012) Free radical scavenging activity, phenolic contents and cytotoxicity of selected Nigerian medicinal plants. Food Chem 131(4):1279–1286
Baghbani-Arani F, Movagharnia R, Sharifian A, Salehi S, Shandiz SAS (2017) Photo-catalytic, anti-bacterial, and anti-cancer properties of phyto-mediated synthesis of silver nanoparticles from *Artemisia tournefortiana* Rchb extract. J Photochem Photobiol B 173:640–649
Bansod SD, Bawaskar MS, Gade AK, Rai MK (2015) Development of shampoo, soap and ointment formulated by green synthesised silver nanoparticles functionalised with antimicrobial plants oils in veterinary dermatology: treatment and prevention strategies. IET Nanobiotechnol 9(4):165–171
Baruah D, Yadav RNS, Yadav A, Das AM (2019) Alpinia nigra fruits mediated synthesis of silver nanoparticles and their antimicrobial and photocatalytic activities. J Photochem Photobiol B Biol 201:111649
Benn T, Cavanagh B, Hristovski K, Posner JD, Westerhoff P (2010) The release of nanosilver from consumer products used in the home. J Environ Qual 39(6):1875–1882
Casañas Pimentel RG, Robles Botero V, San Martín Martínez E, Gómez García C, Hinestroza JP (2016) Soybean agglutinin-conjugated silver nanoparticles nanocarriers in the treatment of breast cancer cells. J Biomater Sci Polym Ed 27(3):218–234
Cui Y, Okyere SK, Gao P, Wen J, Cao S, Wang Y, Deng J, Hu Y (2021) *Ageratina adenophora* disrupts the intestinal structure and immune barrier integrity in rats. Toxins 13(9):651
Dakal TC, Kumar A, Majumdar RS, Yadav V (2016) Mechanistic basis of antimicrobial actions of silver nanoparticles. Front Microbiol 7:1831
Garg VK, Paliwal SK (2011) Wound-healing activity of ethanolic and aqueous extracts of *Ficus benghalensis*. J Adv Pharm Technol Res 2(2):110–114
Gautam SK, Baid Y, Magar PT, Binadi TR, Regmi B (2021) Antimicrobial study of green synthesized silver nanoparticles (AgNPs) by using *Ageratina adenophora* and its characterization. Int J Appl Sci Biotechnol 9(2):128–132
Giri S, Sahu R, Paul P, Nandi G, Dua TK (2022) An updated review on *Eupatorium adenophorum* Spreng. [*Ageratina adenophora* (Spreng)]: traditional uses, phytochemistry, pharmacological activities and toxicity. Pharmacol Res Mod Chin Med 2:100068
Jayapriya M, Dhanasekaran D, Arulmozhi M, Nandhakumar E, Senthilkumar N, Sureshkumar K (2019) Green synthesis of silver nanoparticles using *Piper longum* catkin extract irradiated by sunlight: antibacterial and catalytic activity. Res Chem Intermed 45(6):3617–3631
Kalmantaeva O, Firstova V, Grishchenko N, Rudnitskaya T, Potapov V, Ignatov S (2020) Antibacterial and immunomodulating activity of silver nanoparticles on mice experimental tuberculosis model. Appl Biochem Microbiol 56(2):226–232
Kasithevar M, Saravanan M, Prakash P, Kumar H, Ovais M, Barabadi H, Shinwari ZK (2017) Green synthesis of silver nanoparticles using *Alysicarpus monilifer* leaf extract and its antibacterial activity against MRSA and CoNS isolates in HIV patients. J Interdiscip Nanomed 2(2):131–141
Khazeo P, Mazumder MU, Puro KN, Jyrwa R, Jamir N, Sailo L (2018) In vitro antioxidant activity of methanolic extracts of *Ageratum conyzoides* and *Ageratina adenophora* leaves. In: Mizoram Science Congress 2018 (MSC 2018). Atlantis Press, pp 169–172
Kumar PV, Pammi S, Kollu P, Satyanarayana K, Shameem U (2014) Green synthesis and characterization of silver nanoparticles using *Boerhaavia diffusa* plant extract and their anti bacterial activity. Ind Crops Prod 52:562–566
Kumar D, Kumar G, Das R, Agrawal V (2018) Strong larvicidal potential of silver nanoparticles (AgNPs) synthesized using *Holarrhena antidysenterica* (L.) Wall. bark extract against malarial vector, *Anopheles stephensi* Liston. Process Saf Environ Prot 116:137–148
Kung J-C, Chen Y-J, Chiang Y-C, Lee C-L, Yang-Wang Y-T, Hung C-C, Shih C-J (2018) Antibacterial activity of silver nanoparticle (AgNP) confined mesoporous structured bioactive powder against *Enterococcus faecalis* infecting root canal systems. J Non Cryst Solids 502:62–70
Lallianrawna S, Muthukumaran R, Ralte V, Gurusubramanian G, Kumar NS (2013) Determination of total phenolic content, total flavonoid content and total antioxidant capacity of *Ageratina adenophora* (Spreng.) King & H. Sci Vis 13(4):149–156
Liu Y, Luo SH, Hua J, Li DS, Ling Y, Luo Q, Li SH (2021) Characterization of defensive cadinenes and a novel sesquiterpene synthase responsible for their biosynthesis from the invasive *Eupatorium adenophorum*. New Phytol 229(3):1740–1754
Lombardo PC, Poli AL, Castro LF, Perussi JR, Schmitt CC (2016) Photochemical deposition of silver nanoparticles on clays and exploring their antibacterial activity. ACS Appl Mater Interfaces 8(33):21640–21647
Manandhar S, Luitel S, Dahal RK (2019) In Vitro Antimicrobial activity of some medicinal plants against human pathogenic bacteria. J Trop Med 2019:1895340
Mandal SK, Boominathan R, Parimaladevi B, Dewanjee S, Mandal SC (2005) Analgesic activity of methanol extract of *Eupatorium adenophorum* Spreng. leaves. Indian J Exp Biol 43(7):662–663
Mani S, Natesan K, Shivaji K, Balasubramanian MG, Ponnusamy P (2019) Cytotoxic effect induced apoptosis in lung cancer cell line on *Ageratina adenophora* leaf extract. Biocatal Agric Biotechnol 22:101381
Mensor LL, Menezes FS, Leitão GG, Reis AS, dos Santos TC, Coube CS, Leitão SG (2001) Screening of Brazilian plant extracts for antioxidant activity by the use of DPPH free radical method. Phytother Res: PTR 15(2):127–130
Muthukumaran U, Govindarajan M, Rajeswary M, Hoti SL (2015) Synthesis and characterization of silver nanoparticles using *Gmelina asiatica* leaf extract against filariasis, dengue, and malaria vector mosquitoes. Parasitol Res 114(5):1817–1827
Neupane NP, Karn AK, Mukeri IH, Pathak P, Kumar P, Singh S, Qureshi IA, Jha T, Verma A (2021) Molecular dynamics analysis of phytochemicals from *Ageratina adenophora* against COVID-19 main protease (Mpro) and human angiotensin-converting enzyme 2 (ACE2). Biocatal Agric Biotechnol 32:101924
Noah NM, Ndangili PM (2022) Green synthesis of nanomaterials from sustainable materials for biosensors and drug delivery. Sens Int 3:100166
Priyadarsini KI, Maity DK, Naik G, Kumar MS, Unnikrishnan M, Satav J, Mohan H (2003) Role of phenolic OH and methylene hydrogen on the free radical reactions and antioxidant activity of curcumin. Free Radical Biol Med 35(5):475–484
Qing Y, Cheng L, Li R, Liu G, Zhang Y, Tang X, Wang J, Liu H, Qin Y (2018) Potential antibacterial mechanism of silver nanoparticles and the optimization of orthopedic implants by advanced modification technologies. Int J Nanomed 13:3311–3327
Raghava S, Mbae KM, Umesha S (2021) Green synthesis of silver nanoparticles by *Rivina humilis* leaf extract to tackle growth of Brucella species and other perilous pathogens. Saudi J Biol Sci 28(1):495–503
Rai M, Kon K, Ingle A, Duran N, Galdiero S, Galdiero M (2014) Broad-spectrum bioactivities of silver nanoparticles: the emerging trends and future prospects. Appl Microbiol Biotechnol 98(5):1951–1961
Rajput S, Kumar D, Agrawal V (2020) Green synthesis of silver nanoparticles using Indian Belladonna extract and their potential

antioxidant, anti-inflammatory, anticancer and larvicidal activities. Plant Cell Rep 39(7):921–939
Ren Z, Okyere SK, Wen J, Xie L, Cui Y, Wang S, Wang J, Cao S, Shen L, Ma X (2021) An overview: the toxicity of *Ageratina adenophora* on animals and its possible interventions. Int J Mol Sci 22(21):11581
Ringmichon C, Gopalkrishnan B (2017) Antipyretic activity of *Eupatorium adenophorum* leaves. Int J Appl Biol Pharm 8:1–4
Shaikh W, Chakraborty S, Islam R (2020) Photocatalytic degradation of rhodamine B under UV irradiation using *Shorea robusta* leaf extract-mediated bio-synthesized silver nanoparticles. Int J Environ Sci Technol 17(4):2059–2072
Sharma OP, Dawra RK, Kurade NP, Sharma PD (1998) A review of the toxicosis and biological properties of the genus Eupatorium. Nat Toxins 6(1):1–14
Shi Z, Hu L, Fu J, Sun W, Yue D, Ren Z, Zhong Z, Zuo Z, Hu Y (2019) Chemical separation product of *Ageratina adenophora* essential oil (AAEO) inhibits the inflammation of RAW2647 cells induced by lipopolysaccharide. Xi bao yu fen zi mian yi xue za zhi = Chin J Cell Mol Immunol 35(4):302–306
Tamuly C, Hazarika M, Bordoloi M, Das MR (2013) Photocatalytic activity of Ag nanoparticles synthesized by using *Piper pedicellatum* C. DC fruits. Mater Lett 102:1–4
Tiwary BK, Bihani S, Kumar A, Chakraborty R, Ghosh R (2015) The in vitro cytotoxic activity of ethno-pharmacological important plants of Darjeeling district of West Bengal against different human cancer cell lines. BMC Complement Altern Med 15:22
Treshchalov A, Erikson H, Puust L, Tsarenko S, Saar R, Vanetsev A, Tammeveski K, Sildos I (2017) Stabilizer-free silver nanoparticles as efficient catalysts for electrochemical reduction of oxygen. J Colloid Interface Sci 491:358–366
Uprety Y, Poudel RC, Asselin H, Boon E (2011) Plant biodiversity and ethnobotany inside the projected impact area of the Upper Seti Hydropower Project, Western Nepal. Environ Dev Sustain 13(3):463–492
Verma A, Mehata MS (2016) Controllable synthesis of silver nanoparticles using Neem leaves and their antimicrobial activity. J Radiat Res Appl Sci 9(1):109–115
Wiegand I, Hilpert K, Hancock RE (2008) Agar and broth dilution methods to determine the minimal inhibitory concentration (MIC) of antimicrobial substances. Nat Protoc 3(2):163–175
Zhu Q, Xu S, Wu W, Qi Y, Lin Z, Li Y, Qin Y (2022) Hierarchical hollow zinc oxide nanocomposites derived from morphology-tunable coordination polymers for enhanced solar hydrogen production. Angew Chem Int Ed Engl 61(29):e202205312